Lipid bilayers decorated with photosensitive ruthenium complexes

Bahreman, A.

2

Ruthenium polypyridyl complexes hopping at anionic lipid bilayers *via* a supramolecular bond sensitive to visible light

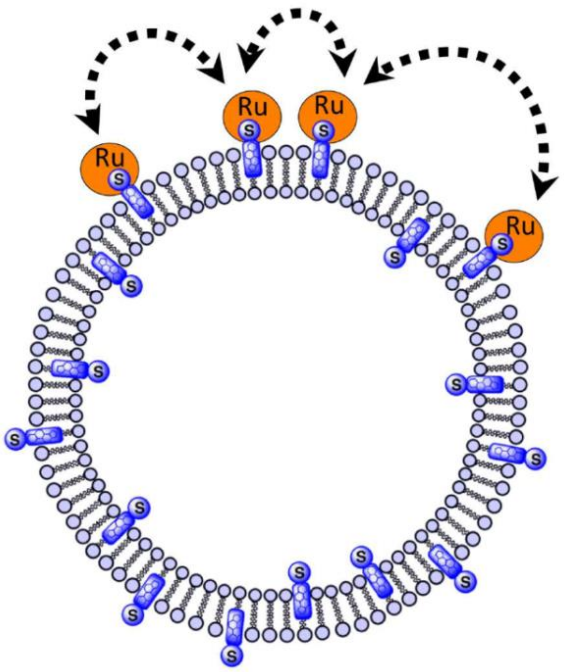

This Chapter has been published as a full paper;
Bahreman, A.; Limburg, B.; Siegler, M.A.; Koning, R.; Koster, A.J.; Bonnet, S.; *Chem. Eur. J.*, **2012**, 18, 10271.

Abstract

The new ruthenium complex [Ru(terpy)(dcbpy)(Hmte)]$(PF_6)_2$ ([**2**]$(PF_6)_2$) was synthesized, where dcbpy is 6,6'-dichloro-2,2'-bipyridine, terpy is 2,2';6',2"-terpyridine, and Hmte is 2-(methylthio)ethanol. The X-ray structure shows that the Ru^{2+} ion is in a distorted octahedral geometry, revealing steric congestion between dcbpy and Hmte. In water, [**2**]$^{2+}$ forms spontaneously by reacting Hmte and the aqua complex [Ru(terpy)(dcbpy)(H_2O)]$^{2+}$ ([**1**]$^{2+}$), with a second-order rate constant of 0.025 $s^{-1}\cdot M^{-1}$ at 297 K. In the dark, the Ru-S bond of [**2**]$^{2+}$ is thermally unstable and partially hydrolyzes; in fact, both complexes [**1**]$^{2+}$ and [**2**]$^{2+}$ are in equilibrium characterized by an equilibrium constant *K* of 151 M^{-1}. By shining visible light at an aqueous solution containing [**2**]$^{2+}$ the Ru-S bond is selectively broken to release [**1**]$^{2+}$, *i.e.*, the equilibrium is shifted by visible light irradiation. Such light-induced equilibrium shifts were repeated four times without signs of major degradation; the Ru-S coordination bond in [**2**]$^{2+}$ can be described as a robust light-sensitive supramolecular bond in water. In order to demonstrate the potential of this system in supramolecular chemistry a new thioether-cholesterol conjugate (**4**) was synthesized that inserts into lipid bilayers via its cholesterol moiety, and coordinates to ruthenium via its sulfur atom. Anionic DMPG lipid vesicles (DMPG=dimyristoylphosphatidylglycerol sodium salt) functionalized with this thioether-conjugate were prepared, to which the aqua complex [**1**]$^{2+}$ efficiently coordinates. Upon visible light irradiation on the Ru-decorated vesicles the Ru-S bond is selectively broken, thus releasing [**1**]$^{2+}$ that stays at the water-bilayer interface. When light is switched off the metal complex spontaneously coordinates back to the membrane-embedded thioether ligands without a need to heat the system. This process was repeated four times at 308 K, thus achieving the light-triggered hopping of the metal complex at the water-bilayer interface.

2.1. Introduction

Shining light onto a chemical system is an attractive way to trigger molecular motion[1-5] or influence self-assembly,[6-8] because it does not modify concentrations. In addition, some chromophores have a very specific absorption band, which makes their photoexcitation very selective and allows for precisely controlling the system. Several light-responsive processes have been used to trigger molecular or supramolecular events, such as the *cis-trans* isomerization of azobenzene,[9-17] alkene,[18-20] or overcrowded alkenes,[21-23] the closing/opening of diarylethenes,[24-28] the cleavage of coordination bonds,[29-34] or the linkage isomerization of transition metal complexes.[35-37] Over the years, light-responsive supramolecular interactions such as that between *trans* azobenzene and cyclodextrin, have led to a particularly large number of applications in nanotechnology, chemical biology, and drug delivery.[38-58]

In this work, a new form of light-responsive supramolecular interaction based on coordination compounds is described. "Supramolecular" specifically means here that the two interacting molecular fragments are involved in a true thermodynamic equilibrium at room temperature, with kinetics occurring at the timescale of minutes to tens of minutes. This equilibrium involves a Ru-S coordination bond that spontaneously forms in aqueous solution and in the dark, but is selectively broken under visible light irradiation.

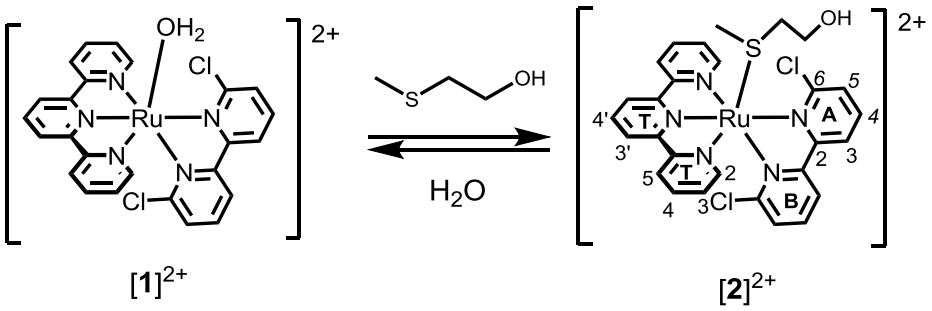

Scheme 2.1. Equilibrium between [**1**]$^{2+}$, Hmte, and [**2**]$^{2+}$ in water.

2.2. Results

2.2.1. Synthesis and X-ray crystal structure

The orange Hmte complex [**2**](PF$_6$)$_2$ was prepared by heating [Ru(terpy)(dcbpy)Cl]Cl ([**3**]Cl)[59] and two equivalents of AgPF$_6$ in Hmte. According to ^{1}H NMR spectroscopy in acetone-d$_6$ the protons of the Hmte ligand are high-field shifted in [**2**](PF$_6$)$_2$ compared to the free ligand, which shows coordination of the ligand to the polypyridyl ruthenium complex. Single crystals suitable for X-ray structure determination were obtained by slow diffusion of diisopropyl ether in an Hmte solution of [**2**](PF$_6$)$_2$. As expected the Hmte ligand coordinates *via* its soft sulfur atom to ruthenium(II) (see Figure 2.1). The ruthenium center is in a distorted octahedral environment, typical for terpy-bound complexes. Noteworthy the dcbpy ligand is positioned out of the plane perpendicular to the terpyridine ligand, with Ru1-N4-C20-C21, Ru1-N5-C21-C20, Ru1-N4-C16-Cl1 and Ru1-N5-C25-Cl2 torsion angles larger than 20°. Such strong distortions, combined with a rather long Ru1-S1 bond distance (2.3819(6) Å), altogether suggest significant steric hindrance between the chloro substituents of dcbpy and the thioether Hmte ligand.[60]

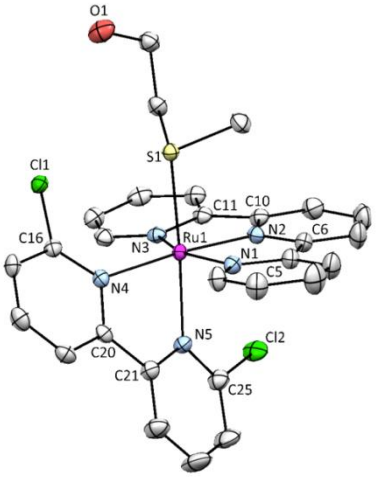

Figure 2.1. Displacement ellipsoid plot (given at 50% probability level) of complex [**2**](PF$_6$)$_2$. Hexafluoridophosphate counter ions and hydrogen atoms have been omitted for clarity. Selected bond length (Å): Ru-S1: 2.3819(6), Ru1-N1: 2.084(2), Ru1-N2: 1.962(1), Ru1-N3: 2.074(2), Ru1-N4: 2.126(2), Ru1-N5: 2.115(2). Selected angles (°): Ru1-N4-C20-C21: 21.5(3), Ru1-N5-C21-C20: 22.0(3), Ru1-N4-C16-Cl1: 23.9(3), Ru1-N5-C25-Cl2: −21.3(3), Ru1-N1-C5-C6: 2.4(3), Ru1-N3-C11-C10: 7.6(3), Ru1-N2-C6-C5: 4.9(3), Ru1-N2-C10-C11: 0.7(3).

2.2.2. Thermodynamics and kinetics in homogeneous aqueous solution

According to ^{1}H NMR the Ru-S bond of [**2**]$^{2+}$ is not stable in water and in the dark. Upon dissolution of [**2**](PF$_6$)$_2$ in D$_2$O two A5 doublets (see Scheme 2.1 for proton notation) at 7.19 and 7.12 ppm reveal the presence of two different ruthenium species in solution (Figure 2.2a). The doublet at 7.19 ppm corresponds to the thioether-bound complex [**2**]$^{2+}$, as it is the most intense signal in the initial spectrum, and as its intensity increases upon addition of free Hmte. The doublet at 7.12 ppm corresponds to the aqua complex [**1**]$^{2+}$, which can be synthesized independently in the form of [**1**](PF$_6$)$_2$ (see Appendix II, section AII.1). Thus, at 297 K the Ru-S bond of [**2**]$^{2+}$ slowly and partially hydrolyses to reach an equilibrium with [**1**]$^{2+}$ and free Hmte. The equiliberium constant *K* was determined by dissolving the chloride complex [**3**]Cl and different amounts of Hmte in D$_2$O (see section 2.4.3 and Figure 2.2a). The Ru-Cl bond of [**3**]$^+$ is indeed quantitatively and rapidly hydrolyzed in D$_2$O to give [**1**]$^{2+}$, as shown by the unique A5 doublet observed at 7.12 ppm upon dissolution of [**3**]Cl in D$_2$O. In presence of different relative amounts of free Hmte and [**3**]Cl, and after equilibration in the dark at 297 K the two expected A5 doublets at 7.19 and 7.12 ppm can be integrated to obtain the relative concentrations in species [**2**]$^{2+}$ and [**1**]$^{2+}$, respectively. A plot of the ratio *[RuHmte]/[RuOH$_2$] vs. [Hmte]* was drawn, where *[RuHmte]*, *[RuOH$_2$]*, and *[Hmte]*, are the concentrations in [**2**]$^{2+}$, [**1**]$^{2+}$, and Hmte, respectively (see Figure 2.2b). A straight line was found, which shows that indeed the reaction shown is Scheme 2.1 is a thermodynamic equilibrium. The slope of this line numerically corresponds to the equilibrium constant *K*; a value of 151(8) M^{-1} was found at 297 K and in the dark.

The kinetics for the coordination of Hmte to [**1**]$^{2+}$ were investigated by UV-vis spectroscopy. Upon adding a large excess of Hmte to an aqueous solution of [**1**]$^{2+}$, the UV-vis spectrum of the solution gradually evolves within minutes in the dark to give a new absorption maximum at 467 nm (Figure AII.1). The clear isosbestic point at 465 nm shows that the coordination of Hmte to ruthenium is selective. In such pseudo first-order conditions the first-order rate constants k'_1 were determined for different concentrations in Hmte (Figure AII.2a). It was found that the order of Hmte in the coordination reaction was one at 297 K (Figure AII.2b), and a value of 0.025(1) M^{-1}·s^{-1} was found for the second-order rate constant k_1. Typically, half-reaction times at room temperature are ~3 min with Hmte concentrations of ~0.2 M. Such reaction rate is several orders of magnitude faster than for comparable systems with the unhindered bpy ligand, which typically react within several hours above 60 °C (see

also Chapter 3).[59, 61] Knowing the equilibrium constant *K* and the rate constant k_1 for the substitution of H_2O by Hmte, the first-order rate constant k_{-1} for the *thermal* substitution of Hmte by water in the dark was calculated to be $1.6(9)\times10^{-4}$ s^{-1} at 297 K (see section 2.4.5). This corresponds to a half-time of 75 min for the spontaneous cleavage of the Ru-S bond of $[\mathbf{2}]^{2+}$ in pure water. Thus, the steric hindrance exerted by the dcbpy chelate on the coordination sphere of the complex not only has an effect on the structure of the Hmte complex $[\mathbf{2}]^{2+}$, as revealed by X-ray crystallography, but also on the rate of formation and cleavage of the Ru-S coordination bond in the dark.

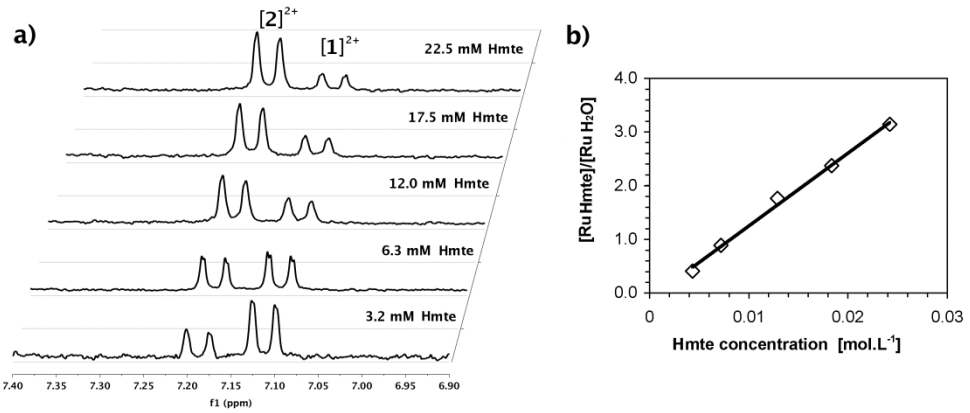

Figure 2.2. a) ^{1}H NMR spectra (A5 region, 7.40-6.90 ppm in D_2O) of equilibrated samples containing $[\mathbf{2}]^{2+}$, $[\mathbf{1}]^{2+}$ and free Hmte; Hmte concentrations are given at t=0 (before equilibration). b) Plot of the *[RuHmte]/[RuOH$_2$]* ratio *vs. [Hmte]*, at the equilibrium and in the dark. Conditions: *T* = 297 K, $[Ru]_{tot}$=2.8 mM.

2.2.3. Photochemistry in homogeneous aqueous solution

Ruthenium polypyridyl complexes like $[Ru(terpy)(bpy)(L)]^{2+}$ are known to selectively photosubstitute the monodentate ligand by a solvent molecule upon visible light irradiation.[29, 62-64] The photoreactivity of this type of complexes is based on the thermal conversion of the photochemically generated ^{3}MLCT state into a dissociative, metal-centered ^{3}MC state. This process is more efficient when the ligand field strength is low, which can be achieved with sterically hindering ligands (see also Chapter 3).[29, 31, 60, 64] The Ru-S bond in $[\mathbf{2}]^{2+}$ was indeed found to be photochemically cleaved by visible light irradiation in water, to form $[\mathbf{1}]^{2+}$. When an aqueous solution of $[\mathbf{2}](PF_6)_2$ was irradiated at 465 nm a faster increase of the absorbance at 500 nm was observed compared to the dark reaction, with a clear isosbestic point at 452 nm (Figure AII-3).

$$r_{photo} = \frac{dn_{RuHmte}}{dt} = k_{\varphi} \cdot n_{RuHmte} \qquad \textbf{(Equation 2.1)}$$

$$k_{\varphi} = \frac{\Phi \cdot \varphi \cdot (1 - 10^{-A_e})}{n_{Ru_{(tot)}}} \qquad \textbf{(Equation 2.2)}$$

The expression of the rate and of the pseudo first-order rate constant k_{φ} of the purely photochemical substitution of Hmte by water is given in Equations 2.1 and 2.2 where n_{RuHmte} is the number of moles of $[\mathbf{2}]^{2+}$ in the cuvette, Φ is the photon flux, φ the photochemical quantum yield of the reaction, A_e the absorbance of the solution at the irradiation wavelength λ_e, and $n_{Ru(tot)}$ the total number of moles of ruthenium in the sample. In this system measuring φ was challenging because of the *a priori* comparable values of k'_1, k_{-1}, and k_{φ} at room temperature (see Chapter 3 for more details). To do so, the solution was irradiated from the top of the UV-Vis cuvette, while absorption spectra were taken from the side, *i.e.*, along the optical axis of the UV-Vis spectrometer (see Figure AI.1). In our experimental conditions a value of 0.097(9) was obtained for the photosubstitution quantum yield φ at 297 K, which is one order of magnitude higher than for comparable unhindered bpy complexes.[61] Such a high efficiency is consistent with previous studies in pyridine,[60] which had shown that steric hindrance on the spectator diimine chelates increased the photosubstitution quantum yield of Ru(II) polypyridyl complexes. Although the Ru-S bond of $[\mathbf{2}]^{2+}$ is thermally not stable in water the photochemical cleavage of the Ru-S bond is typically one order of magnitude faster than the thermal reaction (see Chapter 3, Table 3.4).

The fast kinetics of the equilibrium shown in Scheme 2.1, coupled to the high photosubstitution quantum yield φ, made us envision that the bimolecular equilibrium between $[\mathbf{1}]^{2+}$ and $[\mathbf{2}]^{2+}$ may be shifted by visible light irradiation in an aqueous solution containing an excess of free Hmte. White light irradiation was thus realized inside a ^{1}H MAS NMR spectrometer on a sample containing $[\mathbf{1}]^{2+}$, $[\mathbf{2}]^{2+}$, and Hmte in D_2O, initially equilibrated at 297 K. Before irradiation, the ^{1}H MAS NMR spectrum of the solution showed two A5 doublets at 7.16 and 7.08 ppm, characteristic for the species $[\mathbf{2}]^{2+}$ and $[\mathbf{1}]^{2+}$, respectively. The slightly different values compared to standard solution NMR spectroscopy is due to different setup of the MAS NMR equipment. The *[RuOH$_2$]/[RuHmte]* ratio at the equilibrium in the dark was ~0.24, *i.e.*, the major ruthenium species was for $[\mathbf{2}]^{2+}$. Upon irradiation, the relative intensity of the doublet

at 7.08 ppm increased (Figure 2.3), showing the gradual enrichment of the system in $[\mathbf{1}]^{2+}$ due to the photochemical cleavage of the Ru-S bond. After 30 minutes of irradiation a steady state was obtained, characterized by a *[RuOH$_2$]/[RuHmte]* ratio of 3.4, *i.e.*, a majority of $[\mathbf{1}]^{2+}$. In a second step the lamp was turned off, upon which the sample spontaneously returned to its original state (*[RuOH$_2$]/[RuHmte]* ~ 0.24) within ~30 min. This experiment unequivocally showed that the thermal equilibrium between $[\mathbf{1}]^{2+}$ and $[\mathbf{2}]^{2+}$ can be perturbed by visible light, and that only these two species (as well as free Hmte, visible in the aliphatic region) are present during and after irradiation at room temperature.

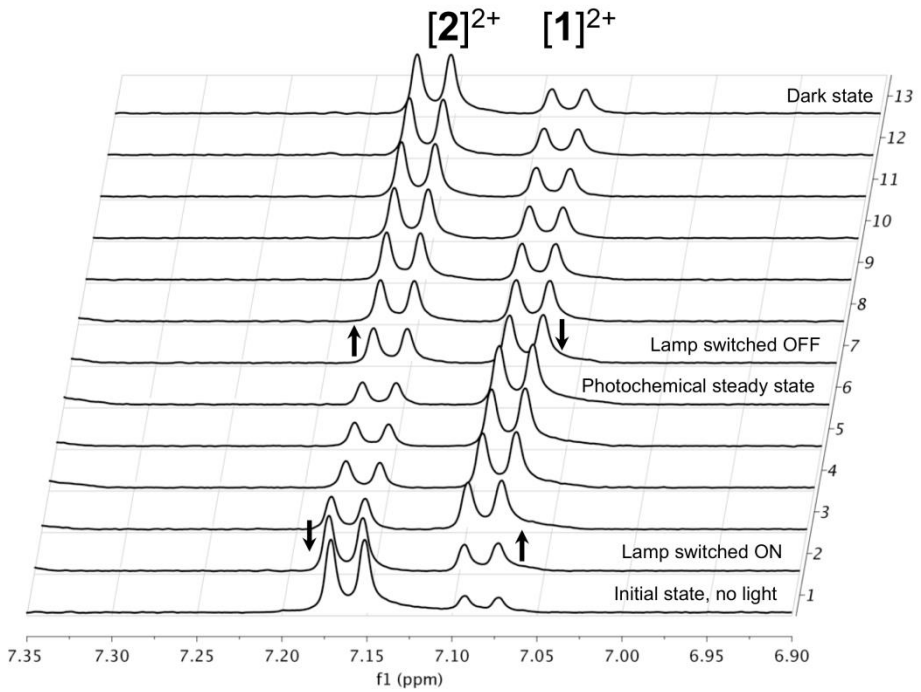

Figure 2.3. Light-induced changes of the equilibrium between $[\mathbf{2}]^{2+}$, $[\mathbf{1}]^{2+}$, and Hmte in water at 298 K, as shown by ^{1}H MAS NMR during white-light irradiation *in situ* (lines 2 to 6) and after switching off the lamp (lines 7 to 13). Spectra taken every 5 minutes.

2.2.4. Repeated shift of a bimolecular equilibrium using light

In order to check whether shifting the equilibrium by light could be repeated several times, further experiments were performed using UV-Vis spectroscopy and

monochromatic (blue) light. An aqueous solution of $[\mathbf{1}]^{2+}$, $[\mathbf{2}]^{2+}$, and Hmte, was prepared and equilibrated at 297 K. In the experimental conditions chosen the composition of the solution was measured to comprise 33% of $[\mathbf{1}]^{2+}$ and 67% of $[\mathbf{2}]^{2+}$ by deconvolution of the UV-vis spectrum. Irradiation at 465 nm was performed 4 times during ~1 h, each time followed by ~2 h of equilibration in the dark. The UV-vis spectra were recorded both under irradiation and in the dark, at 5 minute intervals during 15 h at 297 K. Figure 2.4 shows the evolution of the percentage of the aqua complex $[\mathbf{1}]^{2+}$ *vs.* time. Similar photochemical steady states were obtained all four times, characterized by 75-80% of the aqua complex $[\mathbf{1}]^{2+}$. During each period in the dark an increase of the concentration of the thioether complex $[\mathbf{2}]^{2+}$ was observed, thus showing that the system spontaneously tries to recover its equilibrium state at a $[\mathbf{2}]^{2+}/[\mathbf{1}]^{2+}$ ratio of 2:1. Thus, the combination of ^{1}H NMR and UV-vis analysis shows that this system is rather robust, involving only the four species $[\mathbf{1}]^{2+}$, $[\mathbf{2}]^{2+}$, free Hmte, and water, which interconvert in a repeatable way upon switching on or off a source of visible light. To our knowledge, this is the first demonstration that light-induced ligand substitution reactions on ruthenium(II) can be controlled by light at one and the same temperature, and in a repetitive fashion. In homogeneous solution, the Ru-S bond of complex $[\mathbf{2}]^{2+}$ appears as a light-sensitive supramolecular bond that spontaneously forms in the dark, but is broken by visible light irradiation.

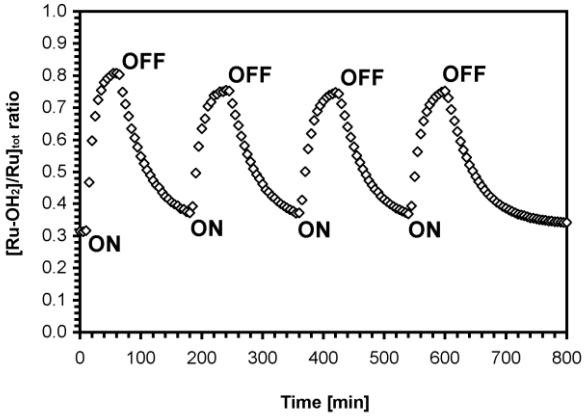

Figure 2.4. Plot of the time evolution of the percentage of $[\mathbf{1}]^{2+}$ in an initially equilibrated homogeneous solution containing $[\mathbf{2}]^{2+}$ and Hmte upon switching ON or OFF several times a source of blue light. Conditions: λ_e = 465 nm, photon flux :3.9×10^{-9} Einstein·s^{-1}, sample temperature 297 K, concentration $[Ru]_{tot}$ = 1.4×10^{-4} M, $[Hmte]$= 9.8×10^{-3} M, spectra measured at 5 minutes interval.

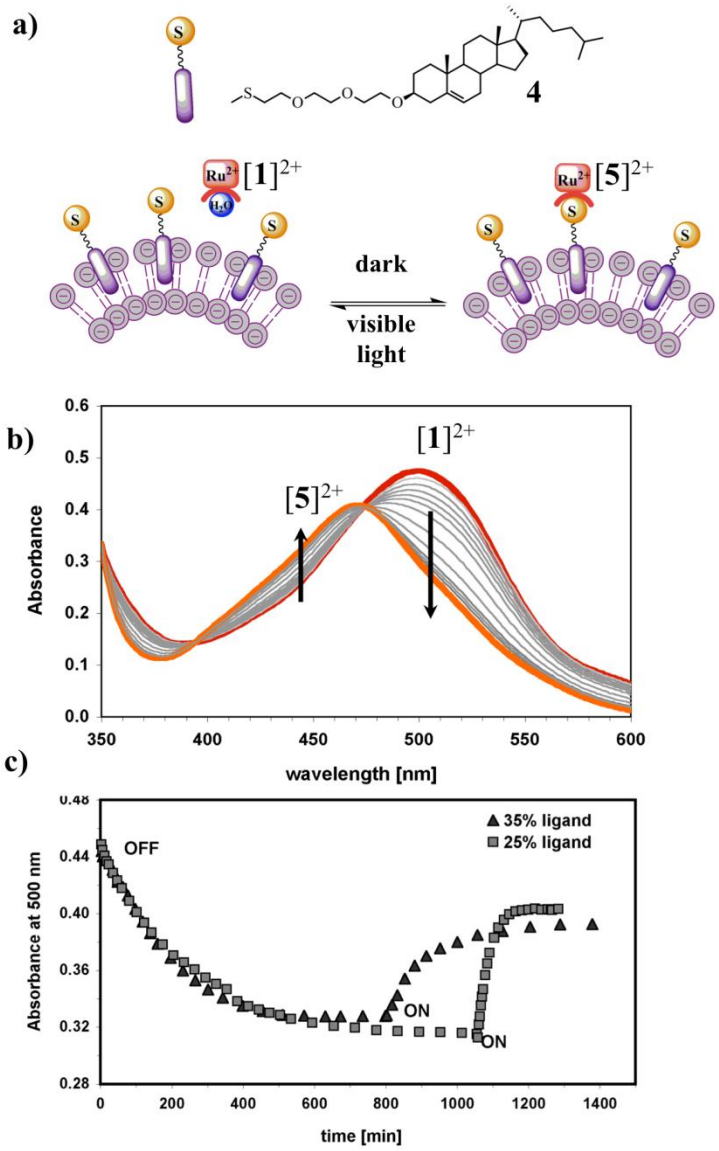

Figure 2.5. a) Scheme showing the chemical structure of **4**, the thermal binding of aqua complex $[\mathbf{1}]^{2+}$ to a lipid bilayer incorporating **4** to give $[\mathbf{5}]^{2+}$, and light-induced unbinding. b) Time evolution of the UV-vis spectrum of a solution containing DMPG vesicles decorated with 25 mol% of ligand **4** after addition of $[\mathbf{1}](PF_6)_2$ at *t*=0, in the dark and at room temperature. c) Time evolution of the absorbance at 500 nm of a solution containing DMPG vesicles functionalized with 25 or 35 mol% of ligand **4** after addition of $[\mathbf{1}](PF_6)_2$ at t=0, in the dark (OFF) and under blue light irradiation (λ_e=465 nm, ON). Condition: T = 297 K, $[Ru]_{tot}$= 6.7 ×10^{-2} mM, [**4**]=0.30 mM (25 mol%) or 0.42 (35 mol%), $[lipid]_{tot}$ = 1.3 mM (as liposomes), photon flux 3.9×10^{-9} Einstein·s^{-1}.

In our quest towards the light-controlled unidirectional motion of individual molecules we considered using this photosensitive Ru-S bond to achieve the light-induced hopping of Ru-based complexes at the surface of (large) unilamellar lipid bilayers. Liposomes represent an appealing system to define an interface where molecular motion can take place: they are easy to synthesize, transparent, and can be further deposited on glass surfaces. In addition, the water-bilayer interface can easily be functionalized using molecular building blocks covalently bound to cholesterol derivatives. Thus, we considered functionalizing liposomes with thioether ligands, and hopping ruthenium complexes at their surface by the repeated dark formation and light-induced cleavage of the Ru-S bond (Figure 2.5a).[61] The thioether-cholesterol conjugate **4** shown in Figure 2.5a was synthesized as described in Appendix II, section AII.1. Large unilamellar anionic DMPG vesicles including 25 mol% or 35 mol% of ligand **4** were prepared by standard extrusion methods; dynamic light scattering measured an average size distribution centered around 140 nm diameter, and cryo-TEM pictures showed the corresponding well-defined, spherical assemblies typical of large unilamellar vesicles (Figure 2.6a).

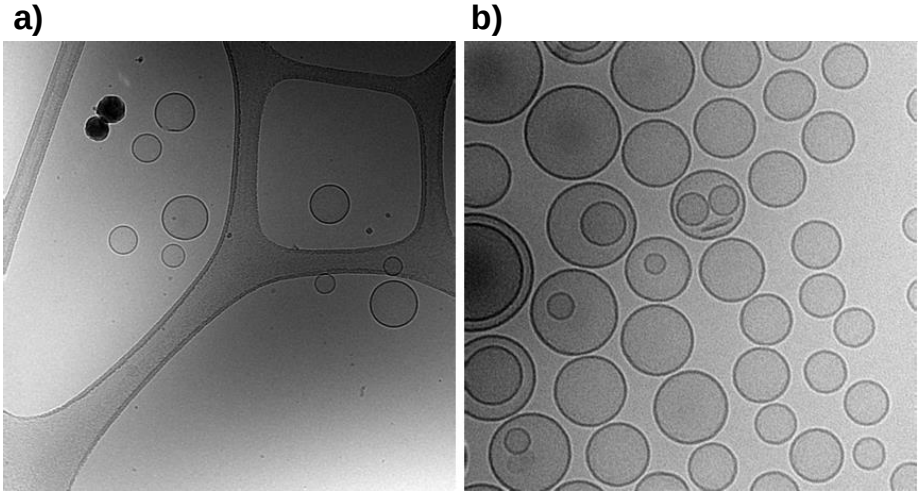

Figure 2.6. Cryo-TEM images of DMPG vesicles decorated with 25 mol% of ligand **4** (a) before and (b) after adding 5 mol% of complex [**1**]$(PF_6)_2$. Images taken at 17000 (a) and 34000 (b) magnification; the size of the whole image is 1.51 μm for (a) and 0.724 μm for (b). Conditions: $[lipid]_{tot}$ = 1.3 mM (as liposomes), vesicle average diameter= 140 nm. Total concentration $[Ru]_{tot}$ = 6.7×10^{-2} mM.

It is shown previously that positively charged aqua ruthenium complexes similar to $[\mathbf{1}]^{2+}$ but containing an unhindered bpy chelate, strongly interact with negatively charged lipid bilayer membranes, and that coordination reaction at membrane-embedded ligands can take place at high temperatures.[61] Knowing that with hindered Ru complexes such as $[\mathbf{1}]^{2+}$ the coordination chemistry is much faster and occurs at room temperature, a solution of $[\mathbf{1}]^{2+}$ was directly added to the thioether-decorated vesicles to observe whether coordination would take place at 297 K. In the dark, the initial absorption maximum of the solution, situated at 496 nm and characteristic of $[\mathbf{1}]^{2+}$ in presence of DMPG liposomes, gradually disappeared to give rise to a new band at 473 nm (Figure 2.5b). The clear isosbestic point at 480 nm shows that a single reaction is taking place. These evolutions are attributed to the formation of the Ru-S complex $[Ru(terpy)(dcbpy)(\mathbf{4})]^{2+}$ (noted $[\mathbf{5}]^{2+}$) at the lipid-water interface (see Figure 2.5a and 2.5b). As $[\mathbf{5}]^{2+}$ is not thermodynamically stable it was not possible to measure its extinction coefficient in the environment of the bilayer as was done for $[\mathbf{2}]^{2+}$ in homogeneous solution. Thus, it was not possible to calculate the final conversion of the coordination reaction. However, from the absence of a shoulder around 500 nm in the last UV-Vis spectrum shown on Figure 2.5b it can be assumed that the conversion is almost complete. Half-reaction times of 165 and 87 min were found for bilayers containing 25 mol% and 35 mol% of ligand **4**, respectively (Figure 2.5c). Thus, like for homogeneous solutions a higher concentration of thioether ligands at the DMPG membrane leads to shorter reaction times. Cryo-TEM images of the samples after adding $[\mathbf{1}]^{2+}$ and equilibration in the dark resembles that taken before addition of ruthenium (Figure 2.6b), showing that the morphology of the vesicles is not modified by the presence and coordination of the ruthenium complex.

After reaching the thermal equilibrium at room temperature the sample was irradiated from the top with blue light (λ_e = 465 nm), and the evolution of the system was followed by UV-vis spectroscopy (Figure 2.5c). For both vesicle samples the absorbance at 500 nm gradually increased, indicating de-coordination of the sulfur ligand from the ruthenium complex and back-formation of the aqua complex $[\mathbf{1}]^{2+}$. Unlike in homogeneous conditions the photosubstitution of the thioether ligand by water was not complete for the sample containing 35 mol% of ligand **4**, and the absorbance at 500 nm when the photochemical steady state was reached was lower than for the sample containing 25 mol% of ligand **4(**see Figure 2.5c). In other words, although $[\mathbf{1}]^{2+}$ predominates in both cases at the photochemical steady state, thermal

binding of $[\mathbf{1}]^{2+}$ to the membrane-embedded ligand may occur also during irradiation. Considering the kinetic results in homogeneous solution (see above), at higher concentration of **4** in the bilayer the rate of the thermal coordination should be higher, hence the $[RuOH_2]/[Ru]_{tot}$ ratio and the absorbance of the solution at 500 nm at the photochemical steady state are expected to be lower. Finally, the photosubstitution quantum yield at the membrane was measured for the sample containing 25 mol% ligand **4** (see Figure AII.4), and a value of 0.065(6) was found, which is consistent with the value found in homogeneous solution.

2.2.5. The coordination reactions occur at the surface of the bilayer

As recently shown for unhindered ruthenium complexes,[61] the positively charged ruthenium complexes $[\mathbf{5}]^{2+}$ and $[\mathbf{1}]^{2+}$ were expected to stay in proximity of the DMPG membrane, whether bound or not to the membrane-embedded thioether ligand. In order to prove this, complex $[\mathbf{1}]^{2+}$ was added to DMPG vesicles including 25 mol% of ligand **4**, and the sample was equilibrated at room temperature. In a second step, the large unilamellar vesicles (LUVs) were filtered using an Amicon centrifugal filter device, to yield an almost colorless filtrate and orange vesicles on the filter. This orange color indicates the presence of complex $[\mathbf{5}]^{2+}$ at the lipid vesicles, whereas according to ICP-OES (Inductively Coupled Plasma Optical Emission Spectroscopy) only 3% of the initially added ruthenium was found in the colorless filtrate. These 3% may correspond to the amount of non-coordinated aqua ruthenium complexes $[\mathbf{1}]^{2+}$ remaining when the equilibrium with $[\mathbf{5}]^{2+}$ is obtained, although it cannot be fully excluded that filtration slightly perturbs the chemical equilibrium at the vesicle surface. To check whether the Ru-DMPG interaction required the presence of the thioether ligand at the bilayer surface the same experiment was performed with DMPG vesicles functionalized with 25 mol% of simple cholesterol, *i.e.*, anionic membranes deprived of thioether ligand. After equilibration at room temperature and filtration with the Amicon device the filtrate showed 12% of the ruthenium initially present in the sample according to ICP-OES, whereas the filter was stained with red-colored lipid vesicles. Thus, even in absence of coordinating thioether ligands a large fraction (88%) of the aqua complex interacts with the bilayer, *i.e.*, the "free" aqua complex $[\mathbf{1}]^{2+}$ stays close to the bilayer surface. In a control experiment, zwitterionic 1,2-dimyristoyl-*sn*-glycero-3-phosphocholine (DMPC) vesicles were prepared containing 25 mol% of ligand **4** or cholesterol. After adding $[\mathbf{1}]^{2+}$ and equilibration overnight both samples were filtered on the Amicon device, to leave a colorless residue in the filter and an intense red color

in the filtrate indicating the presence of $[\mathbf{1}]^{2+}$. According to ICP-OES the Ru concentration in the filtrate was found to be 96 and 90% of the initial Ru concentration in presence and in absence of coordinating thioether ligands, respectively. Thus, with neutral DMPC vesicles there is a negligible interaction between $[\mathbf{1}]^{2+}$ and the lipid bilayer, whether thioether ligands are embedded in the membrane or not. Overall, these results confirm that the interaction between polypyridyl Ru(II) complexes and DMPG membranes is based on electrostatic forces, and that the coordination chemistry between the aqua complex $[\mathbf{1}]^{2+}$ and the thioether ligands takes place at the negatively charged surface of the lipid bilayer (see Chapter 4).

2.2.6. Hopping of a ruthenium complex at the surface of a lipid bilayer

In order to check whether the results observed in homogeneous solution would stay valid for a supramolecular system the thermal binding and light-induced unbinding of Ru^{2+} at the surface of anionic DMPG lipid bilayers were repeated at 35 °C using a sample containing 35 mol% of ligand **4** and 5 mol% of complex $[\mathbf{1}]^{2+}$. The sample, initially equilibrated in the dark, was irradiated for 1 h at 465 nm and left in the dark for 2 h four consecutive times, while UV-vis spectra were recorded at 3-minute intervals. The time evolution of the absorbance at 500 nm is shown in Figure 2.7. Isosbestic points were obtained for each irradiation and each dark period, showing the selectivity of all reactions. A slow increase of the baseline was observed, which is attributed to water evaporation over long reaction times at 308 K. In the experimental setup indeed the UV-vis cell was left open to allow for irradiation from the top of the cuvette. A high absorbance at 500 nm was observed at the end of each irradiation period, showing the presence of a majority of $[\mathbf{1}]^{2+}$; reversely, a low absorbance at 500 nm was found in the end of each dark period, showing the presence of a majority of $[\mathbf{5}]^{2+}$. According to all results above, the ruthenium complex $[\mathbf{1}]^{2+}$ hops from coordination site to coordination site at the water-bilayer interface. This motion is triggered by visible light.

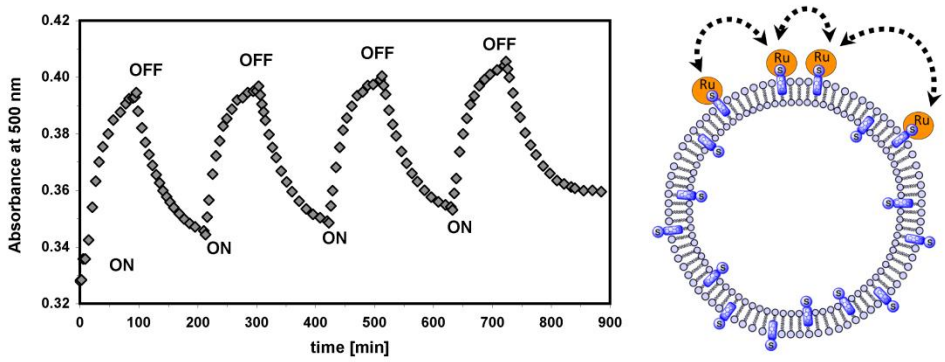

Figure 2.7. Left: Time evolution of the absorbance at 500 nm of an equilibrated solution initially containing DMPG vesicles functionalized with 35 mol% of ligand **4** and 5 mol% of [**1**](PF$_6$)$_2$. At t=0 the sample is alternatively irradiated with blue light (λ_e=465 nm, ON) or left in the dark (OFF). Right: representation of the light-induced hopping of a Ru complex on DMPG lipid bilayer. Conditions: T = 308 K, $[lipid]_{tot}$ = 1.3 mM (as liposomes), vesicle average size= 140 nm, total concentration $[Ru]_{tot}$ = 6.7×10^{-2} mM , spectra measured every 3 minutes, photon flux ~3.9×10^{-9} Einstein·s^{-1}. Absorbance baseline due to light scattering at the vesicles was removed.

2.3. Discussion and conclusion

The effects of steric hindrance on the photo- and thermal reactivity of polypyridyl ruthenium complexes has been studied by Sauvage[29, 60] and Takeuchi,[59, 65] respectively. The photoreactivity of this type of complexes, based on the generation of a ^{3}MC state with strong dissociative character,[62-63] is efficient only if the ligand field strength is low enough, which can be achieved by using sterically hindered ligands. Very often however, steric hindrance also hinders thermal coordination of the photocleaved ligand back to the metal, and the system must be heated to recover its initial photoreactive state.[1, 31, 61, 66] In this work, we show that in contrast to previous photoresponsive systems the steric hindrance of the dcbpy chelate destabilizes both the aqua- and the thioether-bound ruthenium complexes. Such destabilization leads to these two complexes being in thermal equilibrium at room temperature and in the dark. In these conditions the destabilization of the aqua complex [**1**]$^{2+}$ is strong enough to lead to the spontaneous formation of thioether complexes such as [**2**]$^{2+}$ or [**5**]$^{2+}$ in water. Meanwhile, the photoreactivity of the thioether complexes is high enough to allow for the selective cleavage of the Ru-S bond upon visible light irradiation, thus

shifting the equilibrium towards a steady state where the ruthenium complex is in majority bound to water.[67] Upon switching off the light, the equilibrium in favor of the thioether-bound complexes is re-established, typically within 30 to 120 minutes at room temperature, and whether the metal complex is in homogeneous solution or adsorbed at lipid bilayers.

In the latter case, the unique combination of the cationic complex $[\mathbf{1}]^{2+}$, a negatively charged lipid bilayer, and a thioether-cholesterol ligand such as **4**, results in the repeated hopping of the photosensitive metal complex at the water-membrane interface without a need to heating the system. Due to the excellent selectivity of both photochemical and thermal ligand substitution reactions, such hopping was repeated four times without alteration of the dark equilibrium state, or of the photochemical steady state. Thus, sterically hindered metal complexes such as $[\mathbf{1}]^{2+}$ might allow for controlling with light the motion of individual molecules.

To conclude, this work shows that the Ru-S coordination bond between $[\mathbf{1}]^{2+}$ and thioether ligands in water is truly supramolecular, *i.e.*, it involves a thermodynamical equilibrium that is established within minutes to hours at room temperature and in the dark. In addition, the sensitivity of this equilibrium to visible light irradiation is not accompanied by secondary degradation processes. To our knowledge only a small number of robust supramolecular interactions is sensitive to visible light and compatible with water; they are all based on the isomerization of covalent double bonds.[6-7, 25] The present work adds a new member in the toolbox of self-assembly in water, which consists in a bimolecular equilibrium that can be shifted by visible light.

2.4. Experimental section

2.4.1. General

^{1}H and ^{13}C NMR spectra were recorded using a Bruker DPX-300 spectrometer; chemical shifts are indicated in ppm relative to TMS. Electrospray mass spectra were recorded on a Finnigan TSQ-quantum instrument using an electrospray ionization technique (ESI-MS). UV-vis spectra were obtained on a Perkin-Elmer Lambda 900 spectrophotometer, or on a Cary Varian UV-visible spectrometer. Liposomes size distributions were determined by dynamic light scattering (DLS) in a Zetasizer (Malvern Instruments Ltd.,U.K.) operated at 633 nm. 2-Dimyristoyl-*sn*-glycero-3-phosphoglycerol sodium salt (DMPG), 1,2-dimyristoyl-*sn*-glycero-3-phosphocholine (DMPC) were obtained from Avanti Polar Lipids

and stored at −18 °C. 6,6'-dibromo-2,2'-bipyridine[68] and [Ru(terpy)Cl_3][69] were synthesized using literature procedures. [**3**]Cl and [**1**]$(PF_6)_2$ were synthesized by modified literature procedures (see Appendix II, Section AII.1).[70] 2-(Methylthio)-ethanol, PCl_5, $POCl_3$ and $AgPF_6$ were purchased from Sigma-Aldrich and used as such.

2.4.2. Synthesis

[**2**]$(PF_6)_2$: [**3**]Cl (50 mg, 79 μmol) and $AgPF_6$ (75 mg, 300 μmol) were dissolved in Hmte (1 mL). The purple solution was quickly heated to 100 °C. After 5 minutes, the orange solution was filtered to remove insoluble AgCl, after which Et_2O was added to precipitate the compound. The orange/red solid was filtered and recrystalized from hot EtOH to yield [**2**]$(PF_6)_2$ (60 mg, 78%). *^{1}H NMR (300 MHz, Acetone-d6, 298 K,* see Scheme 2.1 for proton notation*)* δ 8.94 (d, J = 8.1 Hz, 1H, B3), 8.87 (d, J = 8.1 Hz, 2H, T3'5'), 8.77 (d, J = 8.1 Hz, 2H, T33"), 8.67 (d, J = 8.1 Hz, 1H, A3), 8.59 – 8.47 (m, 4H, T66"+T4'+B4), 8.34 – 8.23 (m, 3H, B5+T44"), 8.03 (t, J = 8.0 Hz, 1H, A4), 7.77 – 7.70 (m, 2H, T55"), 7.42 (d, J = 8.0 Hz, 1H, A5), 3.52 (t, J = 5.7 Hz, 2H, S-CH_2-C$\underline{H}_2$), 1.76 (t, J = 5.8 Hz, 2H, S-C$\underline{H}_2$), 1.18 (s, 3H, S-$\underline{Me}$). ^{13}C NMR was impossible due to slow decomposition of the product in acetone. *UV-vis:* λ_{max} (ε in $L \cdot mol^{-1} \cdot cm^{-1}$) in pure H_2O: 467 nm (6640). *ES MS m/z (calc):* 650.0 (650.6 [M – 2 PF_6− H]$^+$), 590.0 (590.4 [M – 2 PF_6 − Hmte + MeO]$^+$), 578.0 (577.43 [M – 2 PF_6 − Hmte + H_2O]$^+$]), 558.1 (558.4 [M − 2 PF_6 − Hmte −H]$^+$), 296.4 (295.7 [M – 2 PF_6 + MeOH]$^{2+}$). Anal. Calcd for $C_{28}H_{25}Cl_2F_{12}N_5OP_2RuS$: C, 35.72; H, 2.68; N, 7.44; S, 3.41. Found: C, 34.57; H, 2.51; N, 7.21; S, 3.12. *Crystal growing:* Large single crystals of complex [**2**]$(PF_6)_2$ suitable for X-ray structure determination were grown by vapor diffusion of diisopropylether into a solution of the compound in Hmte (~20 mg in 0.5 mL Hmte).

C*rystal structure data for* [**2**]$(PF_6)_2$: Fw = 941.50, dark orange lath, 0.45 × 0.20 × 0.05 mm^3, triclinic, $P\bar{1}$ (no. 2), a = 8.28578(11), b = 10.46214(12), c = 19.7560(2) Å, α = 87.3323(10), β = 88.7860(10), γ = 84.6069(10)°, V = 1702.92(3) Å^3, Z = 2, D_x = 1.836 g cm^{-3}, μ = 0.873 mm^{-1}, abs. corr. range: 0.764–0.959. 29119 Reflections were measured up to a resolution of $(\sin \theta/\lambda)_{max}$ = 0.59 Å^{-1}. 5991 Reflections were unique (R_{int} = 0.0559), of which 5377 were observed [$I > 2\sigma(I)$]. 531 Parameters were refined with 208 restraints. $R1/wR2$ [$I > 2\sigma(I)$]: 0.0293/0.0698. $R1/wR2$ [all refl.]: 0.0349/0.0716. S = 1.055. Residual electron density found between −0.43 and 0.57 eÅ^{-3}.

2.4.3. Determination of the equilibrium constant K

The equilibrium constant (unit: M^{-1}) for the equilibrium shown in Scheme 2.1 is defined by:

$$K = \frac{[RuHmte]}{[Hmte] \cdot [RuOH_2]}$$

A stock solution of $[\mathbf{1}]^{2+}$ was prepared by dissolving complex [**3**]Cl in D_2O (solution **A**, 10 mg in 5 mL, 2.85 mM); a second stock solution of Hmte in D_2O was prepared (solution **B**, 15 µL Hmte in 1 mL, 163 mM). Five NMR tubes were prepared containing 0.5 mL of solution **A** (1.4 µmol [**3**]Cl). To each NMR tube was added 10 µL, 20 µL, 40 µL, 60 µL, or 80 µL of solution **B** corresponding to initial Hmte concentrations of 3.2, 6.3, 12.0, 17.5 and 22.5 mM, respectively. Each NMR tube was put in a water bath for 30 minutes at 50 °C and left to equilibrate overnight at room temperature. After this NMR spectra were measured at room temperature to determine the relative integral of the two species, and checked by another NMR spectrum to ensure the sample was at equilibrium. A plot of *[RuOH$_2$]/[RuHmte]* as a function of the concentration in Hmte was made to determine the equilibrium constant *K*, where *[RuHmte]* represents the concentration in $[\mathbf{2}]^{2+}$ and *[RuOH$_2$]* the concentration in $[\mathbf{1}]^{2+}$.

2.4.4. Order in Hmte and determination of the second-order rate constant k_1 for the thermal substitution of water by Hmte on complex $[\mathbf{1}]^{2+}$

Stock solutions of complex [**3**]Cl (solution **C**, 7.53 mg in 50 mL H_2O, 2.14×10^{-4} M) and Hmte (solution **D**, 438.10 mg in 10 mL H_2O, 4.75×10^{-1} M) were prepared. For a typical experiment, 2 mL of solution **C** was added to a UV-vis cell, which was placed in a UV-vis spectrometer equipped with temperature control set to 297 K and stirring. To this solution was added *x* mL of H_2O, and $1-x$ mL of solution **D**, where *x* was 0.2 mL, 0.4 mL, 0.6 mL or 0.8 mL. After the addition a UV-vis spectrum was taken every 30 seconds for a total of 6 minutes. For each spectrum *[RuHmte]* and *[RuOH$_2$]*, *i.e.*, the concentrations in $[\mathbf{2}]^{2+}$ and $[\mathbf{1}]^{2+}$, respectively, were determined by deconvolution knowing the extinction coefficients of both species at 440 and 500 nm (ε = 5430 and 3609 $L\cdot mol^{-1}\cdot cm^{-1}$ for $[\mathbf{2}]^{2+}$, respectively, and 4680 and 7130 $L\cdot mol^{-1}.cm^{-1}$ for $[\mathbf{1}]^{2+}$, respectively). The rate constants k'_1 were determined by plotting $ln([RuOH_2]/[Ru]_{tot})$ *vs*. time. Values of 0.000861, 0.00168, 0.00241, and 0.00313 s^{-1} were found for k'_1 for Hmte concentrations of 0.0317, 0.0634, 0.0951, and 0.126 M, respectively. Plotting k'_1 *vs. [Hmte]* afforded a straight line corresponding to a first order for Hmte (Figure AII.2). The slope of this line gives for the second-order rate constant k_1 a value of 0.025 $s^{-1}\cdot M^{-1}$ ($R^2 = 0.995$).

2.4.5. Rate constant for the thermal substitution of Hmte by water on complex $[2]^{2+}$

At the thermodynamic equilibrium between $[\mathbf{1}]^{2+}$, free Hmte, $[\mathbf{2}]^{2+}$, and water, the rates for the formation and hydrolysis of complex $[\mathbf{2}]^{2+}$ are equal:

$$k_{-1} \cdot [RuHmte]_{eq} = k_1 \cdot [RuOH_2]_{eq} \cdot [Hmte]_{eq}$$

Thus the second order rate constant k_{-1} for the thermal substitution of Hmte by water is numerically given by $k_{-1} = \frac{k_1}{K}$

2.4.6. ^{1}H MAS NMR under irradiation

To determine the effect of light on the chemical equilibria, ^{1}H NMR was performed on a Bruker 400 DMX equipped with a MAS probe (Bruker). A sample was prepared by adding to complex [**3**]Cl (3.2 mg, 4.56 µmol) 0.5 mL of a D_2O solution of Hmte (6.7 mg, 72.7 µmol in 2.5 mL). The sample was put in a water bath at 50 °C for 30 minutes and cooled down to room temperature overnight for equilibration. The solution was loaded into a 4 mm clear sapphire rotor and inserted into the MAS probe. ^{1}H NMR spectra (64 scans) were taken every 5 minutes at 298 K with a spinning frequency of 2 kHz in the dark, or under white light irradiation. The light produced by a 1000 W xenon arc lamp equipped with a water filter and an infrared filter was brought perpendicularly to the rotation axis of the rotor through a fiber optic wire. The sample was irradiated during 30 minutes in total, and left in the dark during 60 minutes. *[RuHmte]* and *[RuOH$_2$]*, *i.e.*, the relative concentration in $[\mathbf{2}]^{2+}$ and $[\mathbf{1}]^{2+}$, respectively, were determined by integration of the peaks at 7.16 ppm and 7.08 ppm, respectively. We attribute the slight difference in chemical shift compared to 7.19 and 7.12 ppm, respectively, to the MAS NMR experimental setup that is different from the standard setup used for solution NMR.

2.4.7. Repeatedly shifting the equilibrium by blue light irradiation

To a UV-vis cell containing 2 mL of a water solution of [**3**]Cl (0.214 mM) was added 1 mL of a water solution of Hmte (prepared with 27.15 mg Hmte in 10 mL H_2O, thus *[Hmte]* = 9.82 mM). The cell was mixed and kept closed in the dark overnight for equilibration at 297 K. The cell was put in a UV-vis spectrophotometer equipped with stirring, and a LED light source was adapted that can irradiate the solution from the top (λ_e = 465 nm, $\Delta\lambda_{1/2}$ = 25 nm, photon flux ~3.9×10^{-9} Einstein·s^{-1}, optical path length 3 cm). The lamp was turned on for 1 hour at t = 0, 3, 6, and 9 hours, the rest of the time it stayed switched off. UV-vis spectra were taken at 5 min intervals, either under irradiation or in the dark, for a total of 15 hours. For each spectrum *[RuHmte]* and *[RuOH$_2$]*, *i.e.*, the concentrations in $[\mathbf{2}]^{2+}$ and $[\mathbf{1}]^{2+}$,

respectively, were determined by deconvolution knowing the extinction coefficients of both species at 440 and 500 nm (ε = 5430 and 3609 $L.mol^{-1}\cdot cm^{-1}$ for $[\mathbf{2}]^{2+}$, respectively, and 4680 and 7130 $L\cdot mol^{-1}\cdot cm^{-1}$ for $[\mathbf{1}]^{2+}$, respectively). The ratio *[RuOH$_2$]/[RuHmte]* was finally plotted as a function of time.

2.4.8. Vesicle preparation

DMPG or DMPC lipid and ligand **4** (25 or 35 mol%) were mixed from a chloroform: methanol (4:1) stock solution and dried under a flow of argon for a few hours. They were subsequently placed under vacuum to remove traces of organic solvents. Afterwards the lipid films were hydrated in a chloride-free buffer containing 10 mM of phosphates, and 40 mM of K_2SO_4 (total ionic concentration 50 mM), at pH=7. The final concentration of the lipids was 2.5 mM. The lipid suspensions were freeze-thawed 10 times (from liquid N_2 temperature to +323 °C) and then extruded 11 times (at 323 °C) by using an Avanti mini-extruder through polycarbonate membranes with 200 nm pore diameter. The size of the vesicles before and after adding $[\mathbf{1}]^{2+}$ were distributed between 130 and 150 nm as measured by DLS. The morphology of the vesicles before and after adding $[\mathbf{1}]^{2+}$ were determined by Cryo-transmission Electron microscopy. The samples were stored at 277 °C and used within 6 days.

2.4.9. Vesicle filtration experiments

1.6 mL samples containing either DMPG or DMPC vesicles functionalized with 25 mol% of either cholesterol or ligand **4**, were prepared as above. Each sample was diluted with the buffer (1.0 mL) before complex $[\mathbf{1}]^{2+}$ was added (0.40 mL of a 5.0×10^{-4} M stock solution of $[\mathbf{1}](PF_6)_2$, to reach a total volume of 3 mL, and final concentrations of 1.3 mM for the lipids and 6.7×10^{-5} M for Ru. The samples were stirred overnight at room temperature and in the dark. Absorbance maxima were measured at 500 nm for both DMPC samples and for the DMPG sample containing cholesterol, which corresponded to the presence of $[\mathbf{1}]^{2+}$. By contrast the absorbance maxima at 473 nm for the sample containing **4** corresponded to the formation of complex $[\mathbf{5}]^{2+}$. In a second step, each sample was centrifuged using a Milipore Ultra-4 centrifugal filter units, at 297 K and 4300 rpm during 90 minutes. The ruthenium concentration of each filtrate was determined by inductively coupled plasma atomic emission spectroscopy (ICP-OES) on a Varian VISTA-MPX spectrometer. The concentrations were found to be 275 ppb and 62 ppb for DMPG samples containing cholesterol and ligand **4**, respectively, and 2.05 and 2.19 ppm for DMPC samples containing cholesterol and ligand **4**, respectively. These values correspond to 12% and 3%

of the initially added Ru for DMPG, and 90% and 96% for DMPC, as the value found for the reference sample was 2.28 ppm (100%).

2.4.10. Irradiation and quantum yield measurement in vesicle samples

1.6 mL of a vesicle sample containing DMPG and 25 mol% of ligand **4** (2.5 mM) was taken in a UV-vis cell. 1 mL of a buffer solution at pH=7 was added and the volume of the cell was completed by adding 0.4 mL of a 5×10^{-4} M stock solution of $[\mathbf{1}]^{2+}$ (ratio $[\mathbf{1}]^{2+}$ to ligand **4** was 1 to 5) . Final lipid concentration in the cell was 1.3 mM. The absorbance of the sample at 500 nm was 0.46. In a second step the sample was stirred in the dark overnight while UV-vis spectra were measured every 3 minutes (Figure AII.4 left). At the thermal equilibrium the absorption maximum was 473 nm, which characterized the formation of complex $[\mathbf{5}]^{2+}$ at the water-bilayer interface, and the absorbance at 473 nm was 0.40. In a third step the sample was irradiated for 90 minutes with a custom-made LED lamp (λ_e = 465 nm, $\Delta\lambda_{1/2}$ = 25 nm) fitted to the top of the UV-vis cell. The absorbance of the solution was measured every 3 minutes during irradiation. Knowing the extinction coefficient and absorbance of $[\mathbf{1}]^{2+}$ at 500 nm (see Appendix I, section AI.1) the extinction coefficient of $[\mathbf{5}]^{2+}$ at 500 nm was calculated to determine the concentration of $[\mathbf{5}]^{2+}$ by deconvolution of each UV-vis spectrum during irradiation. By determining the slope of the plot $ln([RuSRR']/[Ru]_{tot})$ as a function of irradiation time ($4.5(4)\times10^{-3}$ s^{-1} for t<72 min, see Figure AII.4 right) and knowing photon flux at the irradiation wavelength, a quantum yield of 0.065(5) was obtained for the photosubstitution of **4** by water at the bilayer-water interface (see Appendix I, section A.I.3 for quantum yield measurements).

2.4.11. Cryo-electron transmission microscopy

A few microliters of vesicle preparation were applied to glow-discharged lacey carbon EM grids. Excess medium was automatically blotted onto Whatman no. 4 filter paper for 1 to 2 sec. in a controlled environment operated at room temperature and 100% humidity. Subsequently, the specimen was vitrified by plunging into liquid propane/ethane. Samples were stored in liquid nitrogen until use. Grids were mounted in a Gatan 626 cryo holder (Gatan, Pleasanton, U.S.A.) and images were recorded on a Tecnai 20 FEG (FEI Company) operated at 200 keV. Images were recorded at −8 micron under focus on a 2k × 2k camera mounted behind an energy filter (Gatan) operated at a slit width of 20 eV.

2.4.12. Supporting Information

Appendix I: General procedure for the determination of extinction coefficients; calculation the concentrations of reacting species from the UV-vis spectra, and quantum yield.

Appendix II: synthetic procedures for dcbpy, [**3**]Cl, [**1**]$(PF_6)_2$, and for compound **4**; X-ray crystal structure determination procedure; Plots for rate constant and quantum yield measurements.

2.5. References

[1] S. Bonnet, J.-P. Collin, *Chem. Soc. Rev.* **2008**, *37*, 1207-1217.
[2] S. Saha, J. F. Stoddart, *Chem. Soc. Rev.* **2007**, *36*, 77-92.
[3] N. Katsonis, M. Lubomska, M. M. Pollard, B. L. Feringa, P. Rudolf, *Prog. Surf. Sci.* **2007**, *82*, 407-434.
[4] S. Silvi, M. Venturi, A. Credi, *Chem. Commun.* **2011**, *47*, 2483-2489.
[5] P. Ceroni, A. Credi, M. Venturi, V. Balzani, *Photochem. Photobiol. Sci.* **2010**, *9*, 1561-1573.
[6] S. K. M. Nalluri, B. J. Ravoo, *Angew. Chem. Int. Ed.* **2010**, *49*, 5371-5374.
[7] S. K. M. Nalluri, J. B. Bultema, E. J. Boekema, B. J. Ravoo, *Chem. Eur. J.* **2011**, *17*, 10297-10303.
[8] J. W. Li, J. M. A. Carnall, M. C. A. Stuart, S. Otto, *Angew. Chem. Int. Ed.* **2011**, *50*, 8384-8386.
[9] A. Ueno, H. Yoshimura, R. Saka, T. Osa, *J. Am. Chem. Soc.* **1979**, *101*, 2779-2780.
[10] T. Muraoka, K. Kinbara, T. Aida, *Nature* **2006**, *440*, 512-515.
[11] K. Kinbara, T. Aida, *Chem. Rev.* **2005**, *105*, 1377-1400.
[12] T. Hugel, N. B. Holland, A. Cattani, L. Moroder, M. Seitz, H. E. Gaub, *Science* **2002**, *296*, 1103-1106.
[13] S. Shinkai, T. Ogawa, T. Nakaji, Y. Kusano, O. Nanabe, *Tetrahedron Lett.* **1979**, *20*, 4569-4572.
[14] S. Shinkai, T. Minami, Y. Kusano, O. Manabe, *J. Am. Chem. Soc.* **1983**, *105*, 1851-1856.
[15] B. Jousselme, P. Blanchard, N. Gallego-Planas, J. Delaunay, M. Allain, P. Richomme, E. Levillain, J. Roncali, *J. Am. Chem. Soc.* **2003**, *125*, 2888-2889.
[16] H. Y. Jiang, S. Kelch, A. Lendlein, *Adv. Mater.* **2006**, *18*, 1471-1475.
[17] K. Ichimura, S. Oh, M. Nakagawa, *Science* **2000**, *288*, 1624-1626.
[18] T. Muraoka, K. Kinbara, T. Aida, *J. Am. Chem. Soc.* **2006**, *128*, 11600-11605.
[19] E. M. Perez, D. T. F. Dryden, D. A. Leigh, G. Teobaldi, F. Zerbetto, *J. Am. Chem. Soc.* **2004**, *126*, 12210-12211.
[20] D. A. Leigh, J. K. Wong, F. Dehez, F. Zerbetto, *Nature* **2003**, *424*, 174-179.
[21] N. Koumura, R. W. J. Zijlstra, R. A. v. Delden, N. Harada, B. L. Feringa, *Nature* **1999**, *401*, 152-155.
[22] A. C. Coleman, J. M. Beierle, M. C. A. Stuart, B. Macia, G. Caroli, J. T. Mika, D. J. van Dijken, J. W. Chen, W. R. Browne, B. L. Feringa, *Nat. Nanotechnol.* **2011**, *6*, 547-552.
[23] W. R. Browne, B. L. Feringa, *Nat. Nanotechnol.* **2006**, *1*, 25-35.
[24] A. Mulder, A. Jukovic, F. W. B. van Leeuwen, H. Kooijman, A. L. Spek, J. Huskens, D. N. Reinhoudt, *Chem. Eur. J.* **2004**, *10*, 1114-1123.
[25] M. Akazawa, K. Uchida, J. J. D. de Jong, J. Areephong, M. Stuart, G. Caroli, W. R. Browneb, B. L. Feringa, *Org. Biomol. Chem.* **2008**, *6*, 1544-1547.
[26] M. Takeshita, M. Irie, *Tetrahedron Lett.* **1998**, *39*, 613-616.
[27] J. Gan, J. L. Pozzo, F. Vogtle, *Mol. Cryst. Liq. Cryst.* **2005**, *430*, 99-106.

[28] A. Mulder, A. Jukovic, L. N. Lucas, J. van Esch, B. L. Feringa, J. Huskens, D. N. Reinhoudt, *Chem. Commun.* **2002**, 2734-2735.
[29] A.-C. Laemmel, J.-P. Collin, J.-P. Sauvage, *Eur. J. Inorg. Chem.* **1999**, 383-386.
[30] E.-R. Schofield, J.-P. Collin, N. Gruber, J.-P. Sauvage, *Chem. Commun.* **2003**, 188-189.
[31] P. Mobian, J.-M. Kern, J.-P. Sauvage, *Angew. Chem. Int. Ed.* **2004**, *43*, 2392-2395.
[32] J.-P. Sauvage, *Chem. Commun.* **2005**, 1507-1510.
[33] J.-P. Collin, A.-C. Laemmel, J.-P. Sauvage, *New J. Chem.* **2001**, *25*, 22-24.
[34] J.-P. Collin, D. Jouvenot, M. Koizumi, J.-P. Sauvage, *Inorg. Chem.* **2005**, *44*, 4693-4698.
[35] S. Bonnet, J.-P. Collin, J.-P. Sauvage, *Inorg. Chem.* **2006**, *45*, 4024-4034.
[36] P. Coppens, I. Novozhilova, A. Kovalevsky, *Chem. Rev.* **2002**, *102*, 1803-1803.
[37] J. J. Rack, *Coord. Chem. Rev.* **2009**, *253*, 78-85.
[38] Y. Wang, M. Zhang, C. Moers, S. Chen, H. Xu, Z. Wang, X. Zhang, Z. Li, *Polymer* **2009**, *50*, 4821-4828.
[39] G. Wenz, B. Han, A. Muller, *Chem. Rev.* **2006**, *106*, 782-817.
[40] Y. Wang, N. Ma, Z. Wang, X. Zhang, *Angew. Chem. Int. Ed.* **2007**, *46*, 2823-2826.
[41] P. Wan, Y. Jiang, Y. Wang, Z. Wang, X. Zhang, *Chem. Commun.* **2008**, 5710-5712.
[42] H. Murakami, A. Kawabuchi, K. Kotoo, M. Kunitake, N. Nakashima, *J. Am. Chem. Soc.* **1997**, *119*, 7605-7606.
[43] J. Zou, B. Guan, X. Liao, M. Jiang, F. Tao, *Macromolecules* **2009**, *42*, 7465-7473.
[44] Y.-L. Zhao, J. F. Stoddart, *Langmuir* **2009**, *25*, 8442-8446.
[45] G. Pouliquen, C. Amiel, C. Tribet, *J. Phys. Chem. B* **2007**, *111*, 5587-5595.
[46] S. Tamesue, Y. Takashima, H. Yamaguchi, S. Shinkai, A. Harada, *Angew. Chem. Int. Ed.* **2010**, *49*, 7461-7464.
[47] K. Peng, I. Tomatsu, A. Kros, *Chem. Commun.* **2010**, *46*, 4094-4096.
[48] X. Chen, L. Hong, X. You, Y. Wang, G. Zou, W. Su, Q. Zhang, *Chem. Commun.* **2009**, 1356-1358.
[49] H. Niino, A. Yabe, A. Ouchi, M. Tanaka, Y. Kawabata, S. Tamura, T. Miyasaka, W. Tagaki, H. Nakahara, K. Fukuda, *Chem. Lett.* **1988**, 1227-1230.
[50] S. K. M. Nalluri, B. J. Ravoo, *Angew. Chem. Int. Ed. Engl* **2010**, *49*, 5371-5374.
[51] I. Tomatsu, A. Hashidzume, A. Harada, *J. Am. Chem. Soc.* **2006**, *128*, 2226-2227.
[52] J. Liu, G. Chen, M. Guo, M. Jiang, *Macromolecules* **2010**, *43*, 8086-8093.
[53] X. Liao, G. Chen, X. Liu, W. Chen, F. Chen, M. Jiang, *Angew. Chem. Int. Ed.* **2010**, *49*, 4409-4413.
[54] I. Tomatsu, A. Hashidzume, A. Harada, *Macromolecules* **2005**, *38*, 5223-5227.
[55] A. Ueno, Y. Tomita, T. Osa, *Tetrahedron Lett.* **1983**, *24*, 5245-5248.
[56] P. V. Jog, M. S. Gin, *Org. Lett.* **2008**, *10*, 3693-3696.
[57] D. P. Ferris, Y.-L. Zhao, N. M. Khashab, H. A. Khatib, J. F. Stoddart, J. I. Zink, *J. Am. Chem. Soc.* **2009**, *131*, 1686-1688.
[58] G. Chen, M. Jiang, *Chem. Soc. Rev.* **2011**, *40*, 2254-2266.
[59] C. A. Bessel, J. A. Margarucci, J. H. Acquaye, R. S. Rubino, J. Crandall, A. J. Jircitano, K. J. Takeuchi, *Inorg. Chem.* **1993**, *32*, 5779-5784.
[60] S. Bonnet, J.-P. Collin, J.-P. Sauvage, E. R. Schofield, *Inorg. Chem.* **2004**, *43*, 8346-8354.
[61] S. Bonnet, B. Limburg, J. D. Meeldijk, R. J. M. Klein Gebbink, J. A. Killian, *J. Am. Chem. Soc.* **2011**, *133*, 252-261.
[62] J. Van Houten, R. J. Watts, *Inorg. Chem.* **1978**, *17*, 3381-3385.
[63] C. R. Hecker, P. E. Fanwick, D. R. McMillin, *Inorg. Chem.* **1991**, *30*, 659-666.
[64] A.-C. Laemmel, J.-P. Collin, J.-P. Sauvage, *Cr. Acad. Sci. Paris IIc* **2000**, *3*, 43-49.

[65] R. A. Leising, J. S. Ohman, K. J. Takeuchi, *Inorg. Chem.* **1988**, *27*, 3804-3809.
[66] J.-P. Collin, D. Jouvenot, M. Koizumi, J.-P. Sauvage, *Eur. J. Inorg. Chem.* **2005**, 1850-1855.
[67] dummy6-Rudcbpy, **2012**.
[68] X. L. Bai, X. D. Liu, M. Wang, C. Q. Kang, L. X. Gao, *Synthesis* **2005**, 458-464.
[69] R. A. Leising, S. A. Kubow, M. R. Churchill, L. A. Buttrey, J. W. Ziller, K. J. Takeuchi, *Inorg. Chem.* **1990**, *29*, 1306-1312.
[70] C. Che, C. Ho, T. Lau, *J. Chem. Soc. Dalton Trans.* **1991**, 1901-1907.